ELSEVIER

Chemical Geology 192 (2002) 59–79

CHEMICAL GEOLOGY
INCLUDING
ISOTOPE GEOSCIENCE

www.elsevier.com/locate/chemgeo

Correction of common lead in U–Pb analyses that do not report ^{204}Pb

Tom Andersen

Department of Geology, Laboratory for Isotope Geology, University of Oslo, PO Box 1047, Blindern, N-0316 Oslo, Norway

Received 20 November 2001; accepted 11 July 2002

Abstract

The presence of common lead contamination in zircons used for U–Pb geochronology is a potentially serious source of error. Traditionally, common lead is measured by analysis of ^{204}Pb, and the isotopic composition of lead corrected accordingly. Some analytical methods (e.g. LAM-ICPMS) do not report ^{204}Pb. Correction methods are available for such analyses, but these assume that the only source of discordance in a zircon is the presence of common lead. Using such a correction on a lead analysis that contains a discordance component caused by lead loss will invariably lead to overcorrection, and hence to a meaningless, young age. By assuming that the observed $^{206}Pb/^{238}U$, $^{207}Pb/^{235}U$ and $^{208}Pb/^{232}Th$ ratios of a discordant zircon can be accounted for by a combination of lead loss at a defined time, and the presence of common lead of known composition, a correction method can be designed that neither uses ^{204}Pb nor assumes concordance. The method proposed here involves a numeric solution to a set of equations relating the content of radiogenic lead in a zircon or other U/Th-enriched mineral to its total lead content, the amount of common lead present, the age of initial crystallization, the age of lead loss and the amount of lead lost in that process. An estimate for the age of lead loss is needed, but in the absence of prior knowledge of this age, the recalculation procedure can be set up in such a way that the bias in initial age caused by a systematic error in the age of lead loss is minimized. Despite this limitation, the method will give less bias in the corrected ages than alternative correction methods.

Keywords: Geochronology; Uranium–lead; Common lead; Lead isotopes

1. Introduction

The U–Th–Pb system of high U–Pb minerals such as zircon provides us with some of the most versatile, precise and robust geochronometers currently available. Common lead is lead of nonradiogenic origin incorporated into a mineral during its initial formation, in subsequent recrystallization processes or by contamination during analysis. As the presence of even small amounts of unsupported lead in a zircon or other datable mineral will increase its apparent U–Th–Pb ages, the presence of undetected or uncorrected common lead is very detrimental to U–Pb dating. In U–Pb geochronology using thermal or secondary ionization mass spectrometers, the minor, nonradiogenic isotope ^{204}Pb is analysed as a monitor of common lead, and the signals of the

E-mail address: tom.andersen@geologi.uio.no (T. Andersen).

0009-2541/02/$ - see front matter
PII: S0009-2541(02)00195-X

radiogenic isotopes ^{206}Pb, ^{207}Pb and ^{208}Pb are corrected in proportion to their relative abundances in common lead. The use of this correction is critically dependent on precise measurement of ^{204}Pb, which is routine in a thermal or secondary ionization mass spectrometry.

The use of plasma-ionization mass spectrometry with in situ laser-ablation microsampling (LAM-ICPMS) is a new and promising analytical approach to U–Pb dating of U-enriched minerals (e.g. zircon). The method combines the lateral spatial resolution of the ion microprobe with greater speed of analysis and considerably less capital investment. Unfortunately, the method used to compensate for the presence of common lead in thermal or secondary ionization mass spectrometry cannot generally be applied to LAM-ICPMS analyses. This problem arises primarily because the low peak/background ratio of the ^{204}Pb peak is compounded by the ubiquitous presence of Hg in the argon nebulizer gas; ^{204}Hg interferes on ^{204}Pb, while the ^{202}Hg peak is so small that reliable measurement is difficult, if not impossible, and hence an overlap correction of sufficient precision is seldom feasible.

Current methods for common lead correction of such U–Pb analyses make assumptions of ideal concordance of $^{206}Pb/^{238}U$ and $^{207}Pb/^{235}U$ or $^{208}Pb/^{232}Th$ (e.g. Ludwig, 2001), which may not always be justified. In this paper, an alternative approach to common lead correction of U–Pb data is presented, which neither requires knowledge of the amount of ^{204}Pb present, nor assumes that corrected compositions plot on the concordia. This method is thus applicable to U–Pb analyses which do not report ^{204}Pb, and to grains which have suffered lead loss in addition to contamination by common lead.

2. Theoretical background

In a U-bearing mineral, radiogenic lead isotopes (^{206}Pb, ^{207}Pb and ^{208}Pb) will accumulate with time due to radioactive decay of uranium and thorium isotopes. For the ^{238}U–^{206}Pb parent–daughter pair, the growth equation is given by:

$$^{206}Pb_r = {}^{238}U(e^{\lambda_{238}t} - 1)$$

where λ_{238} is the decay constant for ^{238}U, and subscript r denotes radiogenic lead. Similar equations apply to the ^{235}U–^{207}Pb and ^{232}Th–^{208}Pb decay series; decay constants and other relevant data can be found in standard introductory texts (e.g. Faure, 1986; Dickin, 1995).

If the system remains closed and the lead contained in the system (zircon or other U-enriched mineral) is entirely radiogenic in origin, three simple parent–daughter ages can be calculated from U–Th–Pb isotope data:

$$t_{206} = \frac{1}{\lambda_{238}} \ln\left(\frac{^{206}Pb_r}{^{238}U} + 1\right),$$

$$t_{207} = \frac{1}{\lambda_{235}} \ln\left(\frac{^{207}Pb_r}{^{235}U} + 1\right),$$

$$t_{208} = \frac{1}{\lambda_{232}} \ln\left(\frac{^{208}Pb_r}{^{232}Th} + 1\right),$$

where λ_{235} and λ_{232} are the decay constants of ^{235}U and ^{232}Th, respectively.

A fourth age ($t_{7/6}$) can be determined from the relationship between $^{207}Pb/^{206}Pb$ and time:

$$\frac{^{207}Pb_r}{^{206}Pb_r} = \frac{^{235}U}{^{238}U}\left(\frac{e^{\lambda_{235}t} - 1}{e^{\lambda_{238}t} - 1}\right) = \frac{1}{137.88}\left(\frac{e^{\lambda_{235}t} - 1}{e^{\lambda_{238}t} - 1}\right),$$

where the present-day $^{238}U/^{235}U$ is constant at 137.88.

If the zircon has suffered lead loss after its crystallization, a systematic age-discordance pattern will result, in which $t_{208} < t_{206} < t_{207} < t_{7/6} \leq t_{true}$. In the case of lead loss late in the history of the sample, the $t_{7/6}$ age still represents the true crystallization age; for ancient lead loss the $t_{7/6}$ is a minimum estimate of the true age.

However, if nonradiogenic lead is incorporated into the mineral at the time of initial crystallization or in some later event, the lead present in the system is no longer exclusively due to in situ radiogenic accumulation, for example:

$$^{206}Pb = {}^{206}Pb_c + {}^{206}Pb_r = {}^{206}Pb_c + {}^{238}U(e^{\lambda_{238}t} - 1),$$

where $^{206}Pb_c$ is the ^{206}Pb component in the nonradiogienic lead incorporated into the system, known as *common lead*. If common lead is present, the ages

determined from observed U–Th–Pb isotope ratios no longer reflect the crystallization age, for example:

$$t_{206}^{obs} = \frac{1}{\lambda_{238}} \ln\left(\frac{^{206}Pb_r + ^{206}Pb_c}{^{238}U} + 1\right) > t_{206}^{true}$$

The increase in the apparent age of U–Pb systems is illustrated by Fig. 1, which shows the effect of 0.1%, 1% and 2% common lead on the age of a zircon with constant U/Th = 3 as a function of true age. As can be seen, $t_{7/6}$ is strongly affected at all ages; the systematic error induced by 1% common lead in a Proterozoic zircon is 100 Ma or more, and the effect increases towards younger ages. For U/Th = 3, the effect of 1% common lead on t_{208} exceeds that on $t_{7/6}$ for Mesoproterozoic or older zircons. For reasonable U/Th ratios, common lead-contaminated Precambrian zircons of this composition will in general show one of the age sequences: $t_{7/6}>t_{207}>t_{208}>t_{206}>t_{true}$, $t_{7/6}>t_{208}>t_{207}>t_{206}>t_{true}$ or $t_{208}>t_{7/6}>t_{207}>t_{206}>t_{true}$.

In U–Pb geochronology based on thermal ionization (TIMS) or secondary ion (SIMS) mass spectrometry, the minor, nonradiogenic lead isotope ^{204}Pb is measured as a monitor of common lead. Using a model for the isotopic composition of common lead, $^{206}Pb_c$, $^{207}Pb_c$ and $^{208}Pb_c$ can be estimated, and the observed radiogenic isotope ratios corrected accordingly. If ^{204}Pb is not reported, as would normally be the case for quadrupole LAM-ICPMS data, this correction cannot be used.

2.1. The 3D, classical U–Th–Pb concordia

A 3D view of the classical concordia diagram is shown in Fig. 2. An ancient zircon which has suffered neither lead loss nor contamination with common lead will plot on a line in space (the "3D concordia"), which is curved in both $^{206}Pb/^{238}U$–$^{207}Pb/^{235}U$ (i.e. the classical U–Pb concordia) and $^{206}Pb/^{238}U$–$^{208}Pb/^{232}Th$ projections. A zircon of age t_1 and with no common lead, which has lost lead in a subsequent event (at t_2), will plot on the straight line connecting the two points C_1 and C_2, corresponding to concordant lead compositions at t_1 and t_2, respectively.

A zircon of age t_1 which has picked up common lead at the time of crystallization will plot on a line from C_1 towards the composition of common lead, which lies at infinity. A zircon of age C_1 with a given fraction, fc, of common lead will plot at A; lead loss at t_2 will displace its composition along a straight line (AC_2) towards concordant lead composition at age t_2 (i.e. point C_2), to an intermediate composition at A'. The lines C_1A, C_1C_2 and AC_2 define a plane in $^{206}Pb/^{238}U$–$^{207}Pb/^{235}U$–$^{208}Pb/^{232}Th$ space.

Correcting a zircon which contains common lead and which has lost part of its total lead content in a later

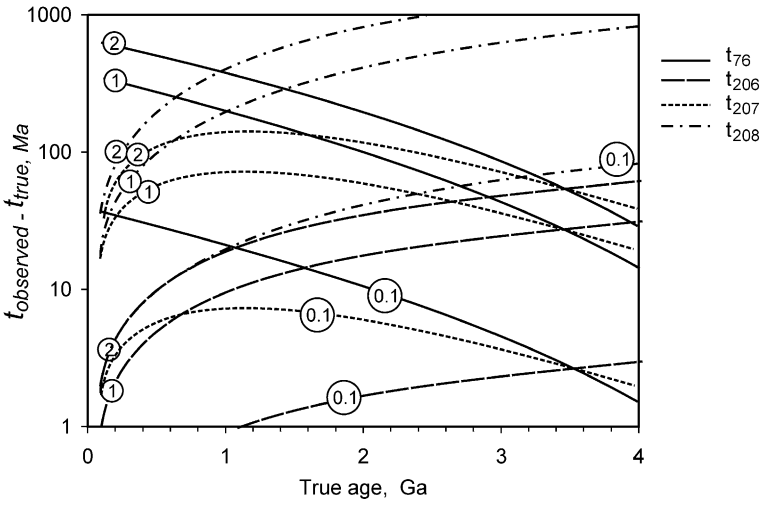

Fig. 1. The change in apparent U–Th–Pb ages induced by contamination with 0.1%, 1% and 2% common lead in a zircon with U/Th = 3, as a function of age. Curves are labeled by the percentage of common lead.

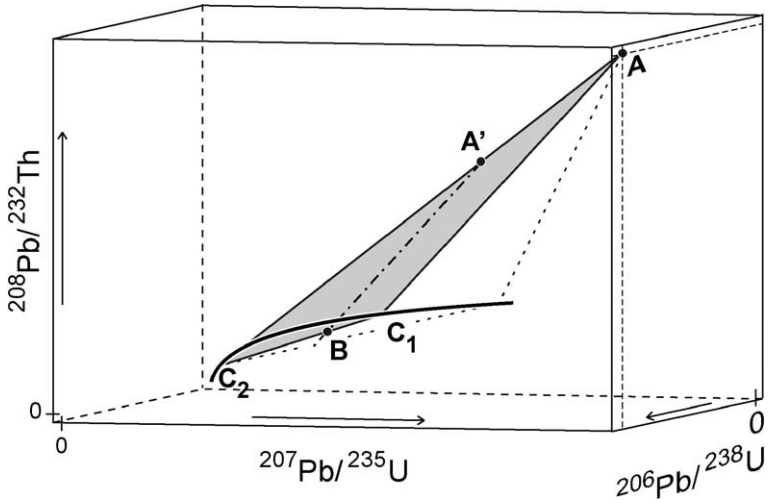

Fig. 2. A 3D view of the classical U–Th–Pb concordia diagram. The concordia is shown as the heavy, curved line starting at the origin. It is terminated at the point where it pierces the arbitrarily chosen front surface of the diagram. Points C_1 and C_2 are concordant lead compositions at times t_1 and t_2, respectively. Point A represents the present-day composition of a zircon of age t_1 with a fraction fc of common ^{206}Pb. Loss of a fraction fl of its total lead at t_2 moves this point to A', which is the analysed composition of the mineral. Correcting for common lead amounts to projecting back along the dash-dot line (defined by A' and the composition of common lead at infinity) to B, which lies at the cord C_1C_2. If the U/Th ratio has not been disturbed, all of these points lie within a single plane in three dimensions, shown by shading. The correction method proposed in this paper determines the position of point B by simultaneous solution of Eqs. (1)–(6). The thin, dotted outline represents a plane hinged on $A'C_2$, which intersects the concordia at $t>t_1$, and which thus cannot include point B or the line $A'B$.

event is equivalent to moving its composition along the line from its measured composition (at A'), along the broken line $A'B$, until intersection with the common lead free lead loss line C_1C_2 at B, which is the radiogenic lead component in the zircon. Since common lead is situated at infinity, this line is fixed in space, parallel with C_1A, and confined to the plane C_1C_2A. For a given t_2, there is only one such plane, and hence only one pair of points C_1 and B. The initial age (t_1, i.e. point C_1), the fraction of lead lost (fl, representing the relative displacement from A to A' or from C_1 to B) and the fraction of common lead (fc, corresponding to the distance from A' to B) are therefore interdependent, and can, in principle, be determined in a single operation. The ^{206}Pb/^{238}U, ^{207}Pb/^{235}U and ^{208}Pb/^{232}Th ratios of a zircon at point B is uniquely given by the composition of concordant lead of age t_1, the age of lead loss (t_2) and the amount of lead lost at t_2.

In geometrical terms, determining the amount of common lead in a zircon which has lost lead amounts to determining the orientation of the plane C_1AC_2. This can be done by making an initial guess of t_1 (as, for example, indicated by the intersection between the concordia and the plane with broken outline in Fig. 2), and rotating this plane with the line AC_2 as a hinge, by reducing t_1, until coincident with the line $A'B$.

3. The correction algorithm

To avoid unnecessarily cluttered equations, a shorthand notation defined in Table 1 is introduced for the derivation of the expressions used to determine the amount of common lead and the error propagation. Let fc be the atomic fraction of common ^{206}Pb in an analysed lead, defined by: $\mathrm{fc} = {}^{206}\mathrm{Pb_c}/{}^{206}\mathrm{Pb} = {}^{206}\mathrm{Pb_c}/({}^{206}\mathrm{Pb_c} + {}^{206}\mathrm{Pb_r})$ where ^{206}Pb$_r$ is the radiogenic lead and ^{206}Pb$_c$ is the common lead. The radiogenic lead component of a common lead-bearing zircon is then given by:

$$y_r = y(1 - \mathrm{fc}) \quad (1)$$

$$x_r = x - yc_7k\mathrm{fc} \quad (2)$$

$$z_r = z - yc_8u\mathrm{fc} \quad (3)$$

Table 1
Parameters used in correction of common lead

Parameter	Standard notation	Shorthand
Radiogenic $^{206}Pb/^{238}U$ ratio	$^{206}Pb_r/^{238}U$	y_r
Radiogenic $^{207}Pb/^{235}U$ ratio	$^{207}Pb_r/^{235}U$	x_r
Radiogenic $^{208}Pb/^{232}Th$ ratio	$^{208}Pb_r/^{232}Th$	z_r
Concordant isotopic ratios at t_1	$^{206}Pb_{t_1}/^{238}U$, $^{207}Pb_{t_1}/^{235}U$, $^{208}Pb_{t_1}/^{232}Th$	y_{t_1}, x_{t_1}, z_{t_1}
Concordant ratios at t_2	$^{206}Pb_{t_2}/^{238}U$, etc.	y_{t_2}, x_{t_2}, z_{t_2}
$^{207}Pb/^{206}Pb$ of common lead	$^{207}Pb_C/^{206}Pb_C$	c_7
$^{208}Pb/^{206}Pb$ of common lead	$^{208}Pb_C/^{206}Pb_C$	c_8
Isotope ratio in present-day uranium	$^{238}U/^{235}U = 137.88$	k
$^{238}U/^{232}Th$ ratio in sample		u
Observed, uncorrected ratios	$^{206}Pb/^{238}U$, $^{207}Pb/^{235}U$, $^{208}Pb/^{232}Th$	y, x, z
Fraction of common ^{206}Pb		fc
Fraction of lead lost at t_2		fl
Real age of zircon (upper intercept age)		t_1
Age of lead loss (known or assumed)		t_2
Error (standard deviation) in parameter a		σ_a
Correlation coefficient of errors in measured $^{206}Pb/^{238}U$ and $^{207}Pb/^{235}U$		ρ
Correlation coefficient of errors in corrected $^{206}Pb/^{238}U$ and $^{207}Pb/^{235}U$		ρ_r

The points C_1, C_2 and B in Fig. 2 are collinear in three dimensions, and must therefore be related by the expressions:

$$\frac{y_r - y_{t_2}}{y_{t_1} - y_{t_2}} = \frac{x_r - x_{t_2}}{x_{t_1} - x_{t_2}} \tag{4}$$

and

$$\frac{z_r - z_{t_2}}{z_{t_1} - z_{t_2}} = \frac{y_r - y_{t_2}}{y_{t_1} - y_{t_2}} \tag{5}$$

The common lead corrected composition is related to the composition of concordant lead at t_1 and t_2 and the fraction of lead lost at t_2:

$$y_r = y_{t_1}(1 - \mathrm{fl}) + y_{t_2}\mathrm{fl} \tag{6}$$

Substituting the composition of radiogenic lead as given by Eqs. (1)–(3) into Eqs. (4) and (5), and eliminating fc from the resulting pair of equations, yields an equation which relates the composition of concordant lead at t_1 (i.e. point C_1 in Fig. 2) to measured composition (A') and the composition of concordant lead of age t_2:

$$\frac{y(x_{t_1} - x_{t_2}) - y_{t_2}x_{t_1} + x(y_{t_2} - y_{t_1}) + x_{t_2}y_{t_1}}{x_{t_1} - x_{t_2} - c_7 k y_{t_1} + c_7 k y_{t_2}} - \frac{z(y_{t_2} - y_{t_1}) + z_{t_2}y_{t_1} + y(z_{t_1} - z_{t_2}) - y_{t_2}z_{t_1}}{z_{t_1} - z_{t_2} - c_8 u y_{t_1} + c_8 u y_{t_2}} = 0 \tag{7}$$

Substituting the relevant expressions for concordant lead compositions at t_1 and t_2 yields an equation which can be solved numerically for t_1. Once t_1 has been determined, the amount of common lead can be calculated from one of the two equivalent expressions for fc which can be derived from Eqs. (4) and (5) above after substitution of the composition of radiogenic lead given by Eqs. (1)–(3), e.g.

$$\mathrm{fc} = \frac{-yx_{t_1} + yx_{t_2} + y_{t_2}x_{t_1} + xy_{t_1} - xy_{t_2} - x_{t_2}y_{t_1}}{-yx_{t_1} + yx_{t_2} + yc_7 k y_{t_1} - yc_7 k y_{t_2}} \tag{8}$$

The composition of the radiogenic lead component in the zircon can then be calculated from Eqs. (1)–(3) above, and the fraction of lead lost at t_2 from the expression:

$$\mathrm{fl} = \frac{y_{t_1} - y_r}{y_{t_1} - y_{t_2}} \tag{9}$$

which is derived from Eq. (6).

3.1. The systematic error introduced by the age of lead loss

The t_1 determined by solving Eq. (7) is dependent on the assumed age of lead loss. The bias introduced by an erroneous choice of t_2 is independent of the amount of common lead removed by the correction algorithm, but

is quite strongly dependent on the amount of lead lost at t_2 (Fig. 3). In general, an underestimate of the age of lead loss (t_2(true) − t_2(assumed)>0) will cause an underestimate of t_1 (t_1(true) − t_1(estimated)>0). As long as the amount of lead lost at t_2 is small (< 5% of the total amount of lead in the case of a mid-Proterozoic zircon having lost lead in the Phanerozoic, Fig. 3a), the estimated t_1 may be expected to deviate from the true t_1 by less than $2\sigma_{t_1}$, even when t_2 is underestimated by as much as 500 Ma. For zircons which are more strongly discordant, the systematic error increases dramatically with the amount of lead lost. The bias is not symmetrical around the true t_2 value; an overestimate of t_2 will lead to a rapidly increasing overestimate of t_1, which is also increasing more rapidly with increasing discordance of the zircon (Fig. 3b). It should be noted that there is an upper limit for t_2, beyond which the method cannot work. This limit is defined by a t_2 for which the point C_2 at the 3D concordia is situated so that the common lead correction line from A' can no longer intersect the chord C_1C_2 (Fig. 2). Assuming a t_2 near this limit may lead to very strongly biased upper intercept ages, or to a situation where Eq. (7) cannot be solved for t_1.

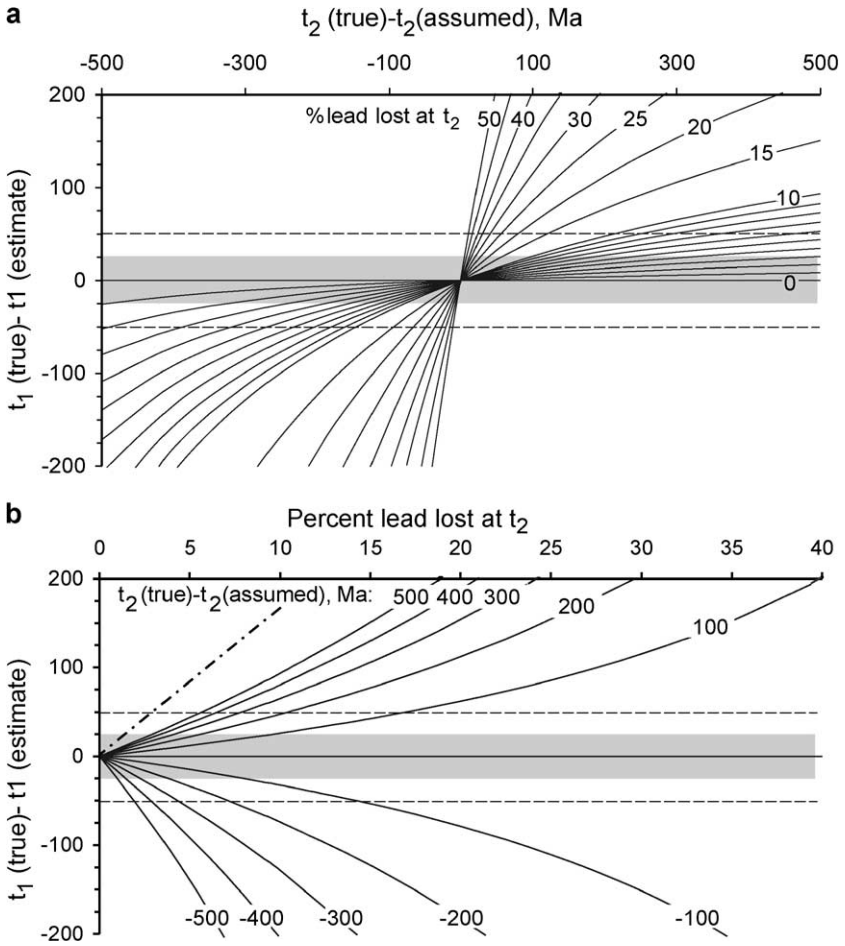

Fig. 3. The effect on the initial age (t_1) of an erroneous choice of age of lead loss (t_2). The model illustrated in this figure is calculated for a 1.5 Ga zircon which has lost lead at 0.5 Ga. The shaded field represents $\pm 1\sigma$ (± 25 Ma) around the "true" age, and the horizontal, broken lines $\pm 2\sigma$. (a) Bias in t_1 as a function of the systematic error in t_2, show for different discordances (in percent). (b) The same situation, shown as a function of discordance, for different systematic errors in t_2. The dash-dot line shows the systematic error caused by applying a ^{207}Pb correction to this zircon.

When the age of lead loss cannot be constrained by independent data, the relationship between systematic errors in t_1 and t_2 illustrated in Fig. 3 suggests that t_2 should be chosen so that the risk of a significant overestimate is minimized. Whereas using $t_2 = 0$ may give meaningful t_1 values for zircons which have lost lead in the early Paleozoic (at least for fl < 5%), the converse is not true: assuming a Paleozoic t_2 for zircons which have suffered recent lead loss could cause a significant overestimate of t_1 even for fl = 1–2%. In any case, zircons, which after correction for common lead appear to have lost more than a few percent of their lead, should be regarded as potentially biased in t_1. The relationship between discordance and systematic error may offer a possible control on the choice of t_2: if a population of zircons with variable fl is corrected at a number of possible t_2, the value likely to cause least systematic error in t_1 will be the one which gives the least systematic change of t_1 with increasing discordance.

3.2. Error propagation

The error in the upper intercept age (t_1) can be estimated by Talyor-expanding Eq. (7) and differentiating the resulting expression for t_1. The resulting expression is quite complicated, but can be calculated numerically. The error in the fraction of common lead can in principle be estimated by substituting concordant lead compositions at t_1 and t_2 and partially differentiating Eq. (8), and adding the contributions in quadrature:

$$\sigma_{\mathrm{fc}} = \sqrt{\left(\frac{\partial \mathrm{fc}}{\partial x}\sigma_x\right)^2 + \left(\frac{\partial \mathrm{fc}}{\partial y}\sigma_y\right)^2 + \left(\frac{\partial \mathrm{fc}}{\partial c_t}\sigma_{c_7}\right)^2 + \left[\left(\frac{\partial \mathrm{fc}}{\partial t_2}\sigma_{t_2}\right)^2\right]} \quad (10)$$

The term in square brackets is invoked if the age of lead loss is supported by data with a statistical error. Otherwise, the effect of an erroneous choice of t_2 introduces a systematic bias which has to be treated separately (Fig. 3). However, the errors in fc and t_1 can more conveniently be estimated by a Monte Carlo simulation routine in which Eqs. (7) and (8) are solved for a large number of random starting compositions, whose x, y and z are compatible with the observed $^{206}Pb/^{238}U$, $^{207}Pb/^{235}U$ and $^{208}Pb/^{232}Th$ ratios, their corresponding errors and the correlation of errors in $^{206}Pb/^{238}U$ and $^{207}Pb/^{235}U$.

Once Eq. (7) has been solved, the U–Th–Pb composition of the radiogenic lead component in the zircon is defined by Eqs. (1)–(3). Corresponding error propagation expressions are derived by partially differentiating the expressions and adding the error contributions in quadrature (e.g. Ludwig, 1980). The error in corrected $^{206}Pb/^{238}U$ depends only on the errors in the observed ratio and the error in the fraction of common lead.

$$\sigma_{y_r} = y_r\sqrt{\left(\frac{\sigma_y}{y}\right)^2 + \left(\frac{\sigma_{\mathrm{fc}}}{1-\mathrm{fc}}\right)^2} \quad (11)$$

On the other hand, the corrected $^{207}Pb/^{235}U$ ratio depends on both of the uncorrected U–Pb isotopic ratios, the errors in the corrected ratio will therefore also be influenced by correlation between errors in $^{206}Pb/^{238}U$ and $^{207}Pb/^{235}U$ (disregarding covariances other than between $^{206}Pb/^{238}U$ and $^{207}Pb/^{235}U$):

$$\sigma_{x_r} = \sqrt{\sigma_x^2 + (\mathrm{fc}\cdot c_7 k)^2\sigma_y^2 + (yc_7k)^2\sigma_{\mathrm{fc}}^2 + (y\mathrm{fc}k)^2\sigma_{c_7}^2 - 2\rho\sigma_x\sigma_y\mathrm{fc}\cdot c_7 k} \quad (12)$$

In contrast, the $^{208}Pb/^{232}Th$ and $^{206}Pb/^{238}U$ ratios do not contain a common divisor and the errors in this pair of ratios are therefore considered as uncorrelated:

$$\sigma_{z_r} = \sqrt{\sigma_z^2 + (\mathrm{fc}\cdot c_8 u)^2\sigma_y^2 + (yc_8u)^2\sigma_{\mathrm{fc}}^2 + (y\mathrm{fc}u)^2\sigma_{c_8}^2 + (y\mathrm{fc}\cdot c_8)^2\sigma_u^2} \quad (13)$$

The correlation coefficient between errors in the corrected $^{206}Pb/^{238}Pb$ and $^{207}Pb/^{235}U$ is given by:

$$\rho_r = \frac{\rho\sigma_x\sigma_y - (\sigma_y/y)^2(\mathrm{fc}\cdot c_7k/x_r) + \sigma_{\mathrm{fc}}^2(y_r c_7 k)/((1-\mathrm{fc})x_r)}{\sigma_{x_r}\sigma_{y_r}} \quad (14)$$

which indicates that the error correlation is reduced by the correction procedure.

Given the errors in the corrected $^{206}Pb/^{238}Pb$ and $^{207}Pb/^{235}U$ ratios and the corresponding error correlation coefficient, the error in corrected $^{207}Pb/^{206}Pb$ is given by:

$$\sigma_{7/6r} = \left(\frac{^{207}Pb}{^{206}Pb}\right)_r \sqrt{\left(\frac{\sigma_{x_r}}{x_r}\right)^2 + \left(\frac{\sigma_{x_r}}{x_r}\right)^2 - 2\rho_r \frac{\sigma_{x_r}}{x_r}\frac{\sigma_{y_r}}{y_r}} \quad (15)$$

The correction algorithm outlined above, including error propagation, has been implemented in a Microsoft Excel template, which can be obtained from the author on request.

4. Discussion

4.1. Comparison with ^{207}Pb and ^{208}Pb corrections

In Fig. 2, the line $A'B$, and hence the path followed by a point during correction for common lead is defined by the position of the analysed, common lead-bearing zircon (at A') and the composition of common lead (at infinity). Hence, this line can only intersect the 3D concordia if fl = 0, i.e. for zircons which have not lost any lead (and for fl = 1, i.e. for zircons which retain no memory of t_1). The alternative correction methods (i.e. the ^{207}Pb and ^{208}Pb corrections, Ludwig, 2001) work with 2D projections of the 3D concordia (Fig. 4). The corrected lead isotope compositions (or corrected $^{207}Pb/^{206}Pb$ ages) are given by the apparent intersections of the relevant projection of the line $A'B$ with the corresponding projection of the concordia, which have real significance only when fl = 0. For zircons which have suffered no lead loss, the ^{207}Pb correction is equivalent to the correction proposed in this paper. Ideally, such zircons are also concordant in $^{208}Pb/^{232}Th$, in which case the ^{208}Pb correction should give identical results. If, however, the zircon has lost lead, the ^{207}Pb correction will give ages which are systematically too low (Fig. 4a). The magnitude of the bias is a function

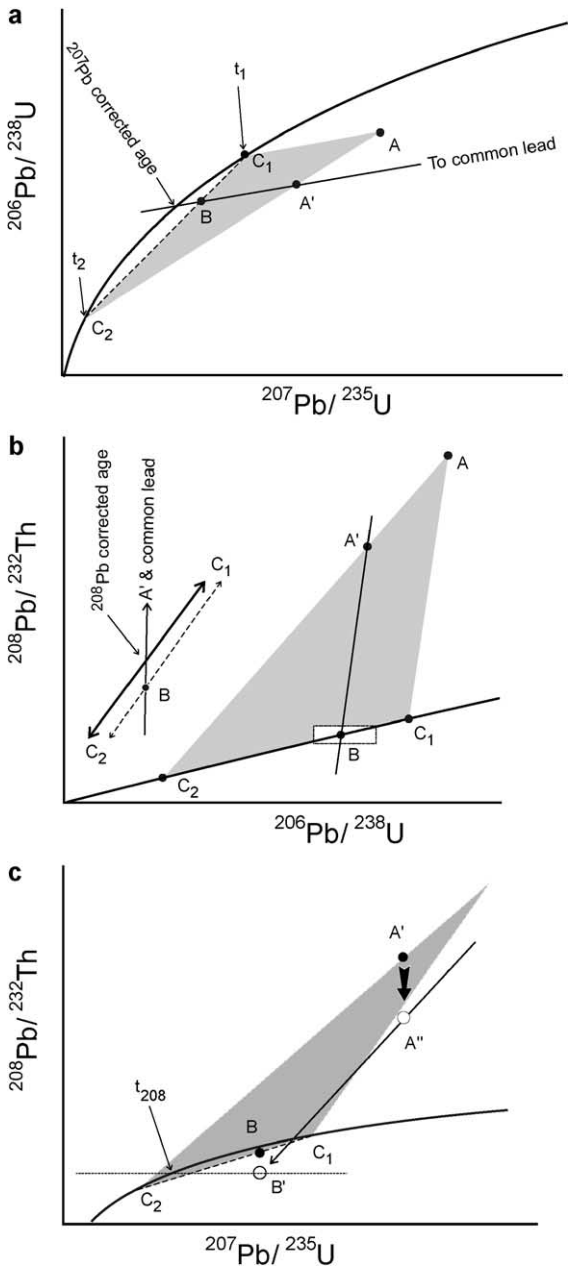

Fig. 4. The present correction method compared to other correction methods, and the effect of U/Th differentiation. See further discussion in the text. (a) Projection of the 3D concordia and the plane $C_1A'C_2$ to the $^{206}Pb/^{238}U$ vs. $^{207}Pb/^{235}U$ plane, i.e. the classical U–Pb concordia diagram. (b) Projection to the $^{208}Pb/^{232}Th$ vs. $^{206}Pb/^{238}U$ plane. Due to the scale of the drawing, the concordia and the chord C_1C_2 appear coincident in the main part of the figure. The detail to the upper left is a magnification of the rectangle around point B. (c) Projection to the $^{208}Pb/^{232}Th$ vs. $^{207}Pb/^{235}U$ plane, showing a case where the U/Th ratio of a zircon has been modified, to displace it out of the plane $C_1A'C_2$ to a point A'' which would correct to B', giving an anomalously low t_{208}.

of the amount of lead lost; Fig. 3 suggests that the bias in the ^{207}Pb corrected age of a mid-Proterozoic zircon, which has lost lead, is of an order of magnitude comparable to that caused by underestimating t_2 by >(>) 500 Ma. Ideally, the ^{208}Pb correction requires a set of processes which induces a discordance in $^{206}Pb/^{238}U$ and $^{207}Pb/^{235}U$, while $^{208}Pb/^{232}Th$ and $^{206}Pb/^{238}U$ remain concordant. Such a scenario may not be very realistic. However, the curvature of the concordia in the $^{208}Pb/^{232}Th$ and $^{206}Pb/^{238}U$ projection (Fig. 4b) is slight, so that the projection of a common lead corrected point at the C_1C_2 chord may overlap within error with the projection of the concordia itself. The corresponding ^{208}Pb corrected age on the 2D $^{208}Pb/^{232}Th$ and $^{206}Pb/^{238}U$ concordia will, however, always be lower than the upper intercept age t_1 (Fig. 4b, detail).

4.2. Zircons whose U/Th ratio has been modified

The U–Th–Pb system can be modified by gain or loss of any of the three elements, lead loss commonly being regarded as the most realistic disturbance (e.g. Lee et al., 1997). Common lead-bearing zircons which have lost or gained Pb, or which have lost or gained U and Th in the same proportion as originally incorporated, will stay within the plane defined by C_1, C_2 and A in Fig. 2 (though not necessarily inside the triangle limited by these points). The true age and the amount and isotopic composition of radiogenic lead fraction in such zircons can in principle be determined from the equations above. However, zircons which are concordant in $^{206}Pb/^{238}U$ and $^{207}Pb/^{235}U$ may be widely discordant in $^{208}Pb/^{232}Th$. The U–Th–Pb systematics of such zircons is best explained in terms of secondary selective gain or loss of Th, most likely due to metamorphic reactions involving a mineral which preferentially incorporates Th (e.g. monazite). If this process is associated with partial loss of lead, the zircon would move out of the plane C_1C_2A (Fig. 2). This shift can be decomposed into a lead-loss component within this plane, and a Th gain or loss vector parallel to the $^{208}Pb/^{232}Th$ axis in Fig. 2 (e.g. from A' to A'' in Fig. 4c). The net effect on t_{208} can be quite dramatic, even in the case of moderate gain or loss of Th (Fig. 4c). The common lead correction line leads to point B' rather than to B on the C_1C_2 chord; in the absence of independent information on how much Th was lost or gained at t_2, this point cannot be corrected back to B.

Zircons which have been affected by U/Th differentiation processes can neither be corrected for common lead by the present method, nor by the ^{208}Pb method. Zircons which have gained significant amounts of Th late in their history can readily be identified from an anomalously low, uncorrected t_{208}; the age sequence $t_{7/6} \geq t_{207} \geq t_{206} \gg t_{208}$ may be a characteristic feature. On the other hand, zircons which have lost thorium may be less easily identified, but will in most cases correct to an inversely discordant radiogenic composition by the present method. Unless reasons for inverse discordance can be inferred from other data, common lead corrected zircons plotting above the concordia should therefore be regarded with due suspicion. The only correction procedure remaining for zircons which have lost or gained Th is the ^{207}Pb correction, which is likely to give a strongly biased age if the zircon has lost lead late in its history (Fig. 3).

4.3. An example

LAM-Q-ICPMS U–Th–Pb data on 107 common lead-bearing zircons are given in Table 2, together with corrected and uncorrected ages. The corrected ages are calculated by the present method at three different t_2, and by the ^{207}Pb and ^{208}Pb correction methods (Ludwig, 2001). The zircons have been separated from mid-Proterozoic calcalkaline orthogneisses from South Norway. From geological constraints, these rocks must have originated as intrusions in a magmatic arc environment between ca. 1600 Ma and the end of subduction in the region at 1500–1510 Ma (e.g. Nordgulen et al., 1997; Sigmond, 1998; Andersen et al., 2001, 2002). The structural fabric and mineralogy of the rocks reflect deformation and metamorphism in Sveconorwegian (i.e. Grenvillian) time, but zircons may also have suffered lead loss in the Phanerozoic (e.g. Bingen and van Breemen, 1998; Connelly and Åhäll, 1996).

Zircons have been corrected for common lead assuming $t_2 = 0$, 250 and 500 Ma. When estimated t_1 is plotted against calculated lead loss, $t_2 = 0$ Ma gives a correlation line with negative slope (Fig. 5a), as predicted for an underestimate of t_2 (cf. Fig. 3). The corresponding correlation line for $t_2 = 500$ Ma suggests

Table 2
LAM-ICPMS data for common lead-bearing zircons from mid-Proterozoic calcalkaline gneisses, South Norway

Analysis	Measured ratios								
	$^{207}Pb/^{206}Pb$	1σ	$^{207}Pb/^{235}U$	1σ	$^{206}Pb/^{238}U$	1σ	$^{208}Pb/^{232}Th$	1σ	$^{238}U/^{232}Th$
108-12	0.0903	0.0010	1.6152	0.0191	0.1295	0.0014	0.1155	0.0015	9.11
108-15	0.1093	0.0023	3.4892	0.0696	0.2333	0.0030	0.1116	0.0025	9.12
108-2	0.1062	0.0013	1.9730	0.0241	0.1347	0.0015	0.0982	0.0012	4.90
108-3	0.0988	0.0012	2.2597	0.0282	0.1658	0.0019	0.0954	0.0012	4.24
108-4	0.0962	0.0010	2.7099	0.0314	0.2042	0.0022	0.1001	0.0012	4.75
108-7	0.2081	0.0023	6.1039	0.0622	0.2127	0.0021	0.4305	0.0042	5.71
108-8	0.1146	0.0013	2.4347	0.0265	0.1541	0.0016	0.0852	0.0009	3.43
110-10	0.1075	0.0013	3.9313	0.0436	0.2652	0.0026	0.0826	0.0009	1.94
110-17	0.1404	0.0015	3.7503	0.0430	0.1937	0.0021	0.0816	0.0009	1.46
110-18	0.1037	0.0013	3.4125	0.0438	0.2387	0.0027	0.0816	0.0010	2.36
110-19	0.1156	0.0013	2.6309	0.0275	0.1648	0.0016	0.1011	0.0010	3.79
110-2	0.1198	0.0013	3.8187	0.0429	0.2312	0.0024	0.1071	0.0011	2.77
110-4	0.0996	0.0013	3.3365	0.0460	0.2421	0.0028	0.0727	0.0009	1.49
110-4	0.0996	0.0013	3.3365	0.0460	0.2421	0.0028	0.0727	0.0009	4.75
110-8	0.1065	0.0012	3.2604	0.0334	0.2220	0.0021	0.0766	0.0008	2.39
FL-10	0.0902	0.0029	2.2678	0.0711	0.1838	0.0028	0.0635	0.0026	5.15
FL-11	0.0980	0.0012	3.5469	0.0492	0.2623	0.0032	0.0781	0.0010	1.62
FL-12	0.0857	0.0010	2.6535	0.0344	0.2245	0.0026	0.0722	0.0011	11.29
FL-14	0.0856	0.0013	2.0619	0.0342	0.1745	0.0022	0.0647	0.0019	20.19
FL-15	0.0998	0.0014	3.3743	0.0523	0.2450	0.0031	0.0796	0.0014	5.15
FL-16	0.0983	0.0011	3.4153	0.0424	0.2519	0.0028	0.0841	0.0010	3.08
FL-17	0.0935	0.0011	3.0443	0.0370	0.2361	0.0026	0.0792	0.0009	4.10
FL-20	0.0957	0.0014	3.0581	0.0486	0.2313	0.0029	0.0801	0.0015	6.56
FL-20CO	0.0911	0.0011	2.7433	0.0353	0.2184	0.0026	0.0783	0.0010	6.80
FL-21	0.0895	0.0011	2.6875	0.0331	0.2180	0.0023	0.0907	0.0012	10.41
FL-23	0.0960	0.0018	1.8583	0.0302	0.1404	0.0012	0.0895	0.0018	7.61
FL-25	0.0936	0.0011	3.0095	0.0364	0.2338	0.0024	0.0799	0.0010	5.14
FL-26	0.0915	0.0011	3.0227	0.0362	0.2398	0.0026	0.0863	0.0012	11.90
FL-8	0.0898	0.0014	2.5260	0.0419	0.2038	0.0026	0.0786	0.0016	7.92
HFG-S-12	0.0949	0.0011	3.1606	0.0393	0.2415	0.0028	0.0763	0.0010	4.14
HFG-S-16	0.0898	0.0011	2.1045	0.0266	0.1700	0.0020	0.0552	0.0007	2.88
HFG-S-17	0.0947	0.0011	3.0243	0.0372	0.2316	0.0026	0.0819	0.0010	3.44
HFG-S-18	0.0927	0.0011	2.4935	0.0302	0.1951	0.0022	0.0779	0.0009	4.00
HFG-S-19	0.0959	0.0012	2.4512	0.0323	0.1857	0.0022	0.0808	0.0010	3.22
HFG-S-20	0.0919	0.0010	2.5819	0.0314	0.2038	0.0023	0.0636	0.0007	2.81
HFG-S-24	0.0868	0.0010	2.5379	0.0325	0.2121	0.0025	0.0653	0.0008	3.56
HFG-S-27	0.0982	0.0012	2.4510	0.0327	0.1806	0.0021	0.0698	0.0009	2.46
HFG-S-28	0.0922	0.0010	2.4994	0.0308	0.1968	0.0023	0.0717	0.0008	2.84
HFG-S-3	0.0937	0.0012	2.4816	0.0325	0.1918	0.0022	0.0807	0.0011	4.69
HFG-S-6	0.0956	0.0012	3.1737	0.0424	0.2408	0.0028	0.0756	0.0010	2.57
HFG-S-8	0.0932	0.0013	3.1216	0.0405	0.2431	0.0025	0.0863	0.0013	9.69
HGG-17	0.0820	0.0026	1.5036	0.0472	0.1330	0.0019	0.1146	0.0067	26.55
HGG-28	0.0824	0.0011	2.2916	0.0342	0.2019	0.0024	0.0643	0.0014	13.70
HGG-7	0.0795	0.0011	2.1374	0.0307	0.1948	0.0021	0.0599	0.0008	2.36
HOM-11	0.1128	0.0022	3.8486	0.0747	0.2489	0.0033	0.1238	0.0025	4.35
HOM-12	0.0935	0.0017	3.2142	0.0597	0.2513	0.0032	0.0770	0.0014	2.79
HOM-13	0.1024	0.0014	3.5132	0.0520	0.2518	0.0031	0.0855	0.0012	3.31
HOM-14	0.0992	0.0012	3.6430	0.0421	0.2677	0.0027	0.0854	0.0010	3.57
HOM-17	0.1153	0.0017	2.7128	0.0427	0.1734	0.0022	0.1041	0.0015	3.61
HOM-18	0.0990	0.0013	3.4876	0.0491	0.2575	0.0031	0.0847	0.0011	2.91
HOM-5	0.0983	0.0016	3.0810	0.0485	0.2292	0.0026	0.0975	0.0017	5.29
HOM-9	0.0987	0.0014	3.4259	0.0470	0.2535	0.0028	0.0775	0.0011	3.58

Table 2 (*continued*)

Analysis	Measured ratios								
	$^{207}Pb/^{206}Pb$	1σ	$^{207}Pb/^{235}U$	1σ	$^{206}Pb/^{238}U$	1σ	$^{208}Pb/^{232}Th$	1σ	$^{238}U/^{232}Th$
JOM-14	0.1030	0.0021	2.9220	0.0587	0.2058	0.0028	0.1037	0.0022	4.49
JOM-15	0.0939	0.0020	2.7299	0.0612	0.2108	0.0031	0.0781	0.0020	6.64
JOM-3	0.0954	0.0014	3.3014	0.0552	0.2515	0.0035	0.0783	0.0013	2.39
JOM-6	0.0981	0.0011	3.3336	0.0483	0.2466	0.0035	0.0816	0.0011	2.67
JUS-11	0.0971	0.0017	3.5397	0.0678	0.2643	0.0039	0.0811	0.0016	4.95
JUS-2	0.1027	0.0014	3.4154	0.0491	0.2413	0.0029	0.0846	0.0012	2.61
JUS-3	0.0944	0.0011	2.9144	0.0373	0.2238	0.0026	0.0691	0.0008	2.92
NES-5	0.0935	0.0010	3.2090	0.0353	0.2491	0.0025	0.0788	0.0009	3.28
NES-14	0.0995	0.0018	3.4933	0.0627	0.2545	0.0032	0.0832	0.0014	3.38
NES-15	0.1087	0.0016	3.9668	0.0541	0.2639	0.0027	0.0948	0.0012	2.70
NES-16	0.0999	0.0013	3.6647	0.0456	0.2661	0.0027	0.0844	0.0011	2.84
NES-19	0.0986	0.0012	3.6001	0.0414	0.2651	0.0027	0.0814	0.0009	2.16
NES-20	0.0964	0.0012	3.4348	0.0421	0.2585	0.0026	0.0787	0.0009	2.67
NES-23	0.0993	0.0013	3.7669	0.0495	0.2754	0.0029	0.0846	0.0012	3.20
NES-24	0.0984	0.0012	3.5788	0.0414	0.2640	0.0027	0.0793	0.0009	2.00
NES-2END	0.0950	0.0010	2.9534	0.0403	0.2253	0.0031	0.0830	0.0011	3.52
NES-3	0.0934	0.0012	2.9759	0.0471	0.2309	0.0034	0.0840	0.0014	4.97
NES-8	0.0986	0.0011	3.2218	0.0448	0.2372	0.0032	0.0924	0.0012	3.91
OE1-1	0.0954	0.0011	3.3771	0.0382	0.2567	0.0027	0.0765	0.0008	2.76
OE1-1	0.0954	0.0011	3.3771	0.0382	0.2567	0.0027	0.0765	0.0008	2.77
OE1-10	0.0965	0.0011	3.3159	0.0436	0.2502	0.0031	0.0781	0.0010	3.71
OE1-10	0.0965	0.0011	3.3159	0.0436	0.2502	0.0031	0.0781	0.0010	3.69
OE1-10B	0.0986	0.0012	3.5001	0.0482	0.2590	0.0033	0.0812	0.0011	3.64
OE1-10B	0.0986	0.0012	3.5001	0.0482	0.2590	0.0033	0.0812	0.0011	3.86
OE1-6	0.0982	0.0011	3.3066	0.0370	0.2440	0.0026	0.0973	0.0010	4.62
OE1-8B	0.1014	0.0011	3.2368	0.0418	0.2331	0.0029	0.0757	0.0009	2.63
OE1-8B	0.1014	0.0011	3.2368	0.0418	0.2331	0.0029	0.0757	0.0009	3.23
OE3-10	0.0953	0.0011	2.5165	0.0341	0.1943	0.0025	0.0647	0.0008	2.86
OE3-16	0.0985	0.0012	3.6678	0.0510	0.2691	0.0034	0.0811	0.0011	2.60
OE3-19	0.0977	0.0011	3.4499	0.0458	0.2552	0.0033	0.0788	0.0010	2.65
OE3-7	0.0985	0.0014	3.3595	0.0485	0.2510	0.0030	0.0763	0.0010	2.40
TA116-15	0.0977	0.0014	3.6071	0.0560	0.2676	0.0036	0.0803	0.0011	1.61
TA116-19	0.1028	0.0012	3.7676	0.0477	0.2659	0.0032	0.0856	0.0010	2.02
TA116-2	0.1023	0.0012	3.6413	0.0498	0.2588	0.0033	0.0800	0.0010	2.27
TA116-24	0.1010	0.0011	3.3332	0.0364	0.2406	0.0025	0.0727	0.0007	2.63
TA116-9	0.1022	0.0015	3.6112	0.0594	0.2563	0.0036	0.0799	0.0012	1.56
TA118-10	0.0977	0.0012	3.4414	0.0416	0.2555	0.0026	0.0792	0.0009	1.58
TA118-14	0.0979	0.0013	3.4478	0.0452	0.2555	0.0028	0.0762	0.0009	1.40
TA118-15	0.1031	0.0015	3.8035	0.0600	0.2665	0.0033	0.0815	0.0012	2.06
TA118-16	0.0978	0.0012	3.4538	0.0453	0.2557	0.0030	0.0766	0.0009	2.23
TA118-17	0.1037	0.0013	3.0864	0.0442	0.2142	0.0026	0.0848	0.0010	2.56
TA118-19	0.1002	0.0012	3.5096	0.0475	0.2536	0.0030	0.0764	0.0009	1.20
TA118-20	0.1005	0.0012	3.4758	0.0410	0.2501	0.0026	0.0763	0.0008	1.59
TA118-4	0.0966	0.0013	3.1931	0.0403	0.2403	0.0023	0.0724	0.0008	1.39
TA118-8	0.0977	0.0016	3.0810	0.0510	0.2287	0.0028	0.0816	0.0013	2.81
TA121-13	0.0947	0.0010	3.0402	0.0391	0.2328	0.0030	0.0791	0.0010	2.95
TA121-16	0.0963	0.0010	3.3467	0.0440	0.2524	0.0034	0.0774	0.0010	2.81
TA121-4	0.0952	0.0011	2.3078	0.0317	0.1761	0.0023	0.0671	0.0009	2.43
TA121-5	0.0892	0.0010	2.2790	0.0285	0.1853	0.0022	0.0597	0.0007	3.64
TA121-6	0.0935	0.0009	3.0800	0.0324	0.2388	0.0025	0.0722	0.0007	3.11
TRO10-4	0.0982	0.0025	3.2949	0.0792	0.2434	0.0029	0.0754	0.0017	3.16

(continued on next page)

Table 2 (*continued*)

Analysis	$t_2=0$					$t_2=250$ Ma				
	% common ^{206}Pb	1σ	Discordance %	Intercept age	1σ	% common ^{206}Pb	1σ	Discordance %	Intercept age	1σ
108-12	3.17	0.09	0	809	35	3.17	0.09	− 3	827	48
108-15	1.01	0.06	− 19	1644	41	1.00	0.06	− 24	1687	47
108-2	4.35	0.13	− 18	1016	39	4.35	0.13	− 31	1097	51
108-3	3.24	0.12	− 3	1045	34	3.24	0.12	− 6	1068	42
108-4	2.01	0.08	0	1223	25	2.01	0.08	− 1	1232	30
108-7	15.05	0.35	− 9	1565	67	15.05	0.35	− 17	1659	78
108-8	3.78	0.12	− 31	1344	30	3.77	0.13	− 44	1460	36
110-10	0.55	0.11	− 11	1687	21	0.54	0.11	− 14	1709	24
110-17	4.79	0.22	− 34	1721	32	4.76	0.22	− 43	1835	35
110-18	1.06	0.11	− 11	1544	25	1.06	0.11	− 15	1570	28
110-19	4.2	0.13	− 23	1298	31	4.19	0.13	− 34	1384	39
110-2	3.13	0.13	− 13	1559	26	3.13	0.13	− 18	1598	30
110-4	0.09	0.05	− 15	1611	23	0.27	0.16	− 17	1611	30
110-4	0.28	0.16	− 13	1584	27	0.08	0.05	− 19	1640	27
110-8	1.13	0.09	− 20	1590	20	1.12	0.09	− 26	1637	24
FL-10	0.47	0.13	− 20	1336	67	0.47	0.13	− 28	1388	80
FL-11	0.15	0.15	− 4	1566	25	0.15	0.15	− 6	1574	28
FL-12	0.11	0.03	− 1	1314	23	0.11	0.03	− 1	1315	27
FL-14	0.18	0.03	− 22	1301	31	0.18	0.03	− 31	1358	38
FL-15	0.31	0.06	− 11	1578	26	0.31	0.06	− 15	1601	31
FL-16	0.66	0.08	− 3	1497	22	0.65	0.08	− 4	1505	25
FL-17	0.49	0.06	− 4	1422	21	0.49	0.06	− 5	1431	25
FL-20	0.39	0.05	− 10	1487	28	0.39	0.05	− 14	1509	33
FL-20CO	0.45	0.04	− 8	1375	22	0.45	0.04	− 11	1393	27
FL-21	0.56	0.03	− 4	1319	24	0.56	0.03	− 5	1329	28
FL-23	2.19	0.09	− 29	1182	45	2.19	0.09	− 43	1287	58
FL-25	0.45	0.05	− 5	1425	23	0.45	0.05	− 7	1437	27
FL-26	0.27	0.02	− 2	1413	22	0.27	0.02	− 3	1417	26
FL-8	0.55	0.05	− 11	1332	31	0.55	0.05	− 15	1357	37
HFG-S-12	0.27	0.06	− 7	1486	21	0.26	0.06	− 9	1500	24
HFG-S-16	0.49	0.09	− 26	1339	23	0.49	0.09	− 36	1413	28
HFG-S-17	0.85	0.08	− 3	1390	22	0.84	0.08	− 4	1399	26
HFG-S-18	1.28	0.08	− 9	1271	24	1.27	0.08	− 14	1297	29
HFG-S-19	2.14	0.11	− 6	1186	30	2.14	0.11	− 10	1210	36
HFG-S-20	0.31	0.08	− 17	1417	21	0.30	0.08	− 23	1456	25
HFG-S-24	0.16	0.07	− 7	1329	22	0.16	0.07	− 10	1344	26
HFG-S-27	1.86	0.13	− 18	1301	30	1.86	0.13	− 26	1355	36
HFG-S-28	1.2	0.1	− 9	1271	24	1.20	0.10	− 13	1296	28
HFG-S-3	1.31	0.08	− 12	1291	26	1.31	0.08	− 18	1326	32
HFG-S-6	0.39	0.1	− 6	1481	24	0.39	0.10	− 9	1494	28
HFG-S-8	0.31	0.03	− 3	1443	26	0.31	0.03	− 4	1450	30
HGG-17	1.03	0.09	− 24	1046	74	1.03	0.09	− 38	1128	98
HGG-28	0.07	0.03	− 5	1239	27	0.07	0.03	− 7	1250	33
HGG-7	0.17	0.1	0	1153	29	0.17	0.10	− 1	1155	35
HOM-11	2.34	0.13	− 4	1523	44	2.34	0.13	− 7	1540	50
HOM-12	0.22	0.11	0	1450	35	0.22	0.11		1451	40
HOM-13	0.71	0.09	− 7	1546	26	0.71	0.09	− 9	1561	30
HOM-14	0.37	0.06	− 1	1547	22	0.37	0.06	− 1	1550	25
HOM-17	4.22	0.16	− 14	1236	44	4.22	0.16	− 23	1293	54
HOM-18	0.61	0.09	− 1	1502	25	0.61	0.09	− 2	1507	28
HOM-5	1.22	0.08	− 4	1390	34	1.22	0.08	− 5	1402	39
HOM-9	0.18	0.07	− 7	1561	25	0.17	0.07	− 10	1575	29

Table 2 (*continued*)

Analysis	$t_2=0$					$t_2=250$ Ma				
	% common ^{206}Pb	1σ	Discordance %	Intercept age	1σ	% common ^{206}Pb	1σ	Discordance %	Intercept age	1σ
JOM-14	2.31	0.13	− 8	1330	48	2.30	0.13	− 12	1358	57
JOM-15	0.56	0.07	− 14	1420	43	0.56	0.07	− 19	1452	51
JOM-3	0.36	0.13	− 2	1477	30	0.36	0.13	− 3	1482	34
JOM-6	0.7	0.11	− 4	1483	23	0.70	0.11	− 6	1493	26
JUS-11	0.14	0.07	− 3	1549	32	0.14	0.07	− 3	1554	37
JUS-2	1.12	0.11	− 8	1515	27	1.12	0.11	− 11	1535	32
JUS-3	0.25	0.08	− 13	1479	22	0.24	0.08	− 17	1507	25
NES-5	0.33	0.07	− 1	1445	20	0.33	0.07	− 1	1448	24
NES-14	0.5	0.1	− 6	1544	34	0.50	0.10	− 7	1556	39
NES-15	1.27	0.1	− 6	1617	28	1.27	0.10	− 9	1633	32
NES-16	0.43	0.08	− 2	1561	24	0.43	0.08	− 3	1566	27
NES-19	0.33	0.1	− 2	1548	22	0.33	0.10	− 3	1553	25
NES-20	0.21	0.08	− 3	1524	23	0.21	0.08	− 4	1530	26
NES-23	0.23	0.08	0	1577	24	0.23	0.08	− 1	1578	28
NES-24	0.19	0.1	− 4	1564	21	0.19	0.10	− 5	1571	24
NES-2END	1.04	0.09	− 4	1367	22	1.04	0.09	− 5	1378	26
NES-3	0.68	0.07	− 3	1390	25	0.68	0.07	− 5	1399	30
NES-8	1.21	0.09	− 2	1413	24	1.21	0.09	− 3	1422	27
OE1-1	0.08	0.07	− 4	1524	19	0.08	0.07	− 5	1531	22
OE1-1	0.08	0.07	− 4	1524	19	0.08	0.07	− 5	1531	22
OE1-10	0.25	0.07	− 5	1513	20	0.25	0.07	− 7	1524	24
OE1-10	0.25	0.07	− 5	1513	20	0.25	0.07	− 7	1523	24
OE1-10B	0.28	0.07	− 4	1546	22	0.28	0.07	− 6	1555	25
OE1-10B	0.26	0.07	− 4	1549	22	0.26	0.07	− 6	1557	25
OE1-6	1.12	0.06	0	1424	21	1.12	0.06	− 1	1428	25
OE1-8B	0.5	0.08	− 15	1568	20	0.61	0.10	− 18	1582	24
OE1-8B	0.61	0.1	− 14	1551	21	0.49	0.08	− 20	1600	23
OE3-10	0.66	0.09	− 20	1404	23	0.66	0.09	− 27	1454	27
OE3-16	0.17	0.1	− 3	1578	22	0.17	0.10	− 4	1584	25
OE3-19	0.29	0.1	− 6	1545	20	0.29	0.10	− 7	1556	23
OE3-7	0.23	0.11	− 6	1535	26	0.23	0.11	− 9	1548	29
TA116-15	0.22	0.17	− 1	1550	29	0.22	0.17	− 2	1553	32
TA116-19	0.75	0.12	− 3	1571	23	0.75	0.12	− 4	1579	26
TA116-2	0.39	0.11	− 8	1609	22	0.38	0.11	− 11	1626	24
TA116-24	0.19	0.08	− 15	1606	19	0.19	0.08	− 19	1636	22
TA116-9	0.64	0.19	− 7	1575	32	0.64	0.19	− 9	1590	35
TA118-10	0.54	0.14	− 2	1502	25	0.54	0.14	− 3	1508	28
TA118-14	0.19	0.15	− 6	1556	26	0.19	0.15	− 8	1569	29
TA118-15	0.35	0.13	− 8	1641	28	0.35	0.13	− 10	1656	31
TA118-16	0.15	0.1	− 7	1564	22	0.15	0.10	− 9	1577	25
TA118-17	2.01	0.13	− 11	1415	29	2.00	0.13	− 16	1447	34
TA118-19	0.39	0.2	− 8	1576	29	0.39	0.20	− 11	1593	32
TA118-20	0.41	0.13	− 10	1581	23	0.41	0.13	− 13	1601	26
TA118-4	0.28	0.15	− 9	1513	26	0.28	0.15	− 12	1532	30
TA118-8	1.11	0.12	− 6	1412	33	1.11	0.12	− 8	1428	39
TA121-13	0.76	0.09	− 4	1404	21	0.76	0.09	− 5	1414	24
TA121-16	0.23	0.09	− 5	1516	19	0.23	0.09	− 6	1525	22
TA121-4	1.75	0.13	− 16	1242	28	1.75	0.13	− 23	1289	34
TA121-5	0.36	0.07	− 20	1349	20	0.35	0.07	− 28	1401	25
TA121-6	0.13	0.07	− 7	1479	17	0.13	0.07	− 10	1494	20
TRO10-4	0.27	0.12	− 10	1551	47	0.27	0.12	− 14	1572	54

(continued on next page)

Table 2 (*continued*)

Analysis	$t_2 = 500$ ma								
	% common ^{206}Pb	1σ	Discordance %	Intercept age	1σ	^{207}Pb corr. (Ma)	1σ	^{208}Pb corr. (Ma)	1σ
108-12	3.17	0.09	− 19	880	88	760	8	756	8
108-15	1.00	0.06	− 33	1753	57	1312	17	1337	16
108-2	5.36	0.17		773	8	773	8	773	9
108-3	3.24	0.12	− 16	1114	61	956	10	952	11
108-4	2.01	0.08	− 4	1247	39	1173	13	1170	12
108-7	15.04	0.36	− 31	1821	95	1041	11	1028	12
108-8	6.05	0.17		871	9	872	9	884	9
110-10	0.54	0.11	− 19	1742	28	1490	15	1508	14
110-17	8.68	0.23		1050	12	1050	11	1082	13
110-18	1.05	0.11	− 21	1610	34	1351	15	1364	15
110-19	5.98	0.17		928	9	929	9	936	9
110-2	3.12	0.13	− 26	1660	36	1282	13	1294	14
110-4	0.08	0.05	− 26	1685	33	1378	16	1395	16
110-4	0.27	0.16	− 23	1652	36	1378	16	1397	15
110-8	1.11	0.09	− 36	1714	29	1255	12	1277	12
FL-10	0.46	0.13	− 41	1479	104	1068	16	1082	15
FL-11	0.15	0.15	− 8	1587	33	1493	18	1500	18
FL-12	0.11	0.03	− 1	1318	35	1304	15	1304	14
FL-14	0.18	0.03	− 46	1463	52	1021	13	1035	12
FL-15	0.31	0.06	− 21	1637	37	1394	17	1408	16
FL-16	0.65	0.08	− 6	1517	30	1434	16	1438	15
FL-17	0.49	0.06	− 8	1446	31	1356	15	1359	14
FL-20	0.39	0.05	− 20	1544	41	1325	16	1336	16
FL-20CO	0.45	0.04	− 17	1422	34	1261	14	1267	14
FL-21	0.56	0.03	− 8	1344	36	1261	13	1263	13
FL-23	3.86	0.19		816	7	816	7	826	7
FL-25	0.45	0.05	− 11	1455	34	1342	14	1347	13
FL-26	0.27	0.02	− 4	1425	32	1380	15	1382	14
FL-8	0.55	0.05	− 23	1401	48	1181	15	1188	14
HFG-S-12	0.26	0.06	− 13	1521	30	1383	16	1391	15
HFG-S-16	2.31	0.14		990	11	990	11	1007	11
HFG-S-17	0.84	0.08	− 7	1414	33	1328	15	1330	14
HFG-S-18	1.27	0.08	− 23	1344	38	1128	12	1132	12
HFG-S-19	2.14	0.11	− 19	1253	48	1070	12	1071	12
HFG-S-20	0.30	0.08	− 33	1523	31	1177	13	1192	13
HFG-S-24	0.16	0.07	− 16	1370	34	1232	14	1238	14
HFG-S-27	1.85	0.13	− 40	1453	47	1039	12	1048	12
HFG-S-28	1.19	0.10	− 21	1339	37	1138	13	1143	13
HFG-S-3	1.31	0.08	− 29	1386	42	1108	12	1115	12
HFG-S-6	0.39	0.10	− 13	1516	34	1378	16	1385	15
HFG-S-8	0.31	0.03	− 6	1460	38	1395	14	1398	13
HGG-17	2.15	0.31		788	11	788	11	795	11
HGG-28	0.07	0.03	− 11	1267	43	1181	14	1185	13
HGG-7	0.17	0.10	− 1	1157	46	1145	12	1145	12
HOM-11	2.34	0.13	− 10	1566	60	1391	18	1396	18
HOM-12	0.22	0.11	− 1	1453	48	1440	18	1442	18
HOM-13	0.71	0.09	− 13	1584	36	1426	17	1436	17
HOM-14	0.37	0.06	− 2	1554	30	1521	15	1523	14
HOM-17	4.21	0.16	− 38	1404	72	976	12	981	13
HOM-18	0.61	0.09	− 3	1514	34	1464	18	1467	17
HOM-5	1.22	0.08	− 9	1421	49	1309	15	1312	14
HOM-9	0.17	0.07	− 14	1597	35	1443	16	1454	15

Table 2 (*continued*)

Analysis	$t_2 = 500$ ma								
	% common ^{206}Pb	1σ	Discordance %	Intercept age	1σ	^{207}Pb corr. (Ma)	1σ	^{208}Pb corr. (Ma)	1σ
JOM-14	2.30	0.13	− 20	1404	72	1171	16	1175	15
JOM-15	0.56	0.07	− 28	1506	64	1213	18	1226	17
JOM-3	0.36	0.13	− 4	1490	40	1438	20	1441	19
JOM-6	0.70	0.11	− 8	1509	31	1405	20	1410	19
JUS-11	0.14	0.07	− 5	1562	44	1506	22	1510	21
JUS-2	1.11	0.11	− 16	1566	38	1367	16	1376	16
JUS-3	0.24	0.08	− 25	1553	31	1285	15	1299	15
NES-5	0.33	0.07	− 2	1451	29	1428	14	1428	14
NES-14	0.50	0.10	− 11	1574	47	1446	18	1454	17
NES-15	1.27	0.10	− 12	1657	38	1480	15	1489	15
NES-16	0.43	0.08	− 5	1575	33	1510	15	1514	15
NES-19	0.33	0.10	− 4	1560	29	1507	15	1510	15
NES-20	0.21	0.08	− 6	1540	32	1475	15	1479	14
NES-23	0.23	0.08	− 1	1581	33	1563	17	1564	16
NES-24	0.19	0.10	− 7	1582	29	1502	15	1508	15
NES-2END	1.03	0.09	− 9	1397	32	1292	17	1295	17
NES-3	0.68	0.07	− 8	1414	37	1327	19	1329	18
NES-8	1.21	0.09	− 6	1436	34	1352	18	1354	17
OE1-1	0.08	0.07	− 7	1542	27	1467	15	1472	14
OE1-1	0.08	0.07	− 7	1542	27	1467	15	1472	14
OE1-10	0.25	0.07	− 10	1540	29	1429	17	1436	17
OE1-10	0.25	0.07	− 10	1539	29	1429	17	1436	17
OE1-10B	0.28	0.07	− 8	1568	30	1474	18	1480	17
OE1-10B	0.26	0.07	− 8	1571	30	1474	18	1481	17
OE1-6	1.12	0.06	− 2	1435	30	1391	15	1390	14
OE1-8B	0.49	0.08	− 27	1651	29	1324	16	1342	16
OE1-8B	0.60	0.10	− 26	1630	29	1324	16	1344	16
OE3-10	0.65	0.09	− 39	1540	34	1119	14	1137	14
OE3-16	0.17	0.10	− 5	1592	29	1530	19	1533	18
OE3-19	0.29	0.10	− 10	1573	28	1454	18	1461	18
OE3-7	0.22	0.11	− 12	1568	35	1429	17	1440	16
TA116-15	0.22	0.17	− 3	1557	37	1523	20	1525	20
TA116-19	0.75	0.12	− 6	1591	30	1503	18	1507	17
TA116-2	0.38	0.11	− 15	1651	29	1465	19	1478	18
TA116-24	0.18	0.08	− 26	1683	27	1367	14	1388	14
TA116-9	0.64	0.19	− 13	1613	41	1451	20	1461	21
TA118-10	0.54	0.14	− 5	1517	33	1455	15	1458	15
TA118-14	0.19	0.16	− 12	1588	34	1455	16	1464	16
TA118-15	0.35	0.13	− 14	1679	37	1506	18	1518	18
TA118-16	0.14	0.10	− 13	1597	30	1457	17	1466	16
TA118-17	2.00	0.13	− 24	1500	42	1217	15	1223	15
TA118-19	0.38	0.20	− 15	1619	37	1440	17	1452	18
TA118-20	0.40	0.13	− 18	1632	30	1420	15	1434	15
TA118-4	0.27	0.15	− 17	1561	36	1373	13	1385	13
TA118-8	1.11	0.12	− 13	1453	47	1307	16	1311	16
TA121-13	0.76	0.09	− 8	1430	29	1335	17	1338	17
TA121-16	0.23	0.09	− 9	1540	27	1441	19	1447	18
TA121-4	1.74	0.13	− 38	1380	44	1017	13	1025	14
TA121-5	0.35	0.07	− 41	1492	33	1078	13	1092	13
TA121-6	0.12	0.06	− 14	1517	25	1370	14	1379	14
TRO10-4	0.26	0.11	− 19	1604	65	1388	17	1401	16

(continued on next page)

Table 2 (*continued*)

Analysis	Corrected ratios, $t_2 = 250$ Ma							
	$^{207}Pb/^{206}Pb$ (Ma)	1σ	$^{207}Pb/^{235}U$ (Ma)	1σ	$^{206}Pb/^{238}U$ (Ma)	1σ	$^{208}Pb/^{232}Th$ (Ma)	1σ
108-12	0.0620	0.0022	1.1428	0.0240	0.1337	0.0014	0.0383	0.0025
108-15	0.0991	0.0025	3.2193	0.0710	0.2356	0.0029	0.0674	0.0034
108-2	0.0669	0.0027	1.2987	0.0325	0.1408	0.0014	0.0389	0.0021
108-3	0.0695	0.0023	1.6411	0.0359	0.1714	0.0018	0.0484	0.0019
108-4	0.0778	0.0018	2.2362	0.0362	0.2083	0.0022	0.0597	0.0019
108-7	0.0700	0.0038	2.4158	0.1078	0.2504	0.0019	0.0531	0.0103
108-8	0.0800	0.0024	1.7659	0.0350	0.1602	0.0015	0.0441	0.0016
110-10	0.1024	0.0016	3.7656	0.0544	0.2667	0.0026	0.0768	0.0014
110-17	0.0959	0.0030	2.6885	0.0649	0.2034	0.0021	0.0538	0.0015
110-18	0.0939	0.0018	3.1216	0.0527	0.2412	0.0027	0.0693	0.0016
110-19	0.0774	0.0023	1.8350	0.0371	0.1720	0.0015	0.0470	0.0019
110-2	0.0907	0.0021	2.9850	0.0529	0.2387	0.0024	0.0657	0.0019
110-4	0.0974	0.0019	3.2600	0.0641	0.2427	0.0028	0.0707	0.0015
110-4	0.0992	0.0015	3.3130	0.0479	0.2423	0.0028	0.0707	0.0015
110-8	0.0961	0.0016	2.9737	0.0406	0.2245	0.0021	0.0643	0.0012
FL-10	0.0852	0.0033	2.1687	0.0764	0.1847	0.0027	0.0543	0.0036
FL-11	0.0967	0.0017	3.5017	0.0661	0.2627	0.0032	0.0768	0.0016
FL-12	0.0848	0.0013	2.6261	0.0349	0.2247	0.0026	0.0666	0.0017
FL-14	0.0841	0.0017	2.0265	0.0346	0.1748	0.0022	0.0518	0.0027
FL-15	0.0970	0.0017	3.2876	0.0547	0.2458	0.0031	0.0716	0.0020
FL-16	0.0923	0.0015	3.2252	0.0477	0.2535	0.0028	0.0736	0.0016
FL-17	0.0890	0.0014	2.9114	0.0400	0.2373	0.0026	0.0694	0.0014
FL-20	0.0923	0.0017	2.9537	0.0503	0.2322	0.0029	0.0678	0.0022
FL-20CO	0.0869	0.0015	2.6296	0.0365	0.2194	0.0025	0.0644	0.0016
FL-21	0.0842	0.0014	2.5463	0.0338	0.2192	0.0023	0.0644	0.0018
FL-23	0.0760	0.0022	1.5045	0.0339	0.1435	0.0012	0.0412	0.0025
FL-25	0.0892	0.0014	2.8880	0.0384	0.2348	0.0024	0.0687	0.0015
FL-26	0.0890	0.0013	2.9493	0.0365	0.2404	0.0026	0.0707	0.0018
FL-8	0.0848	0.0018	2.3960	0.0434	0.2049	0.0026	0.0602	0.0022
HFG-S-12	0.0925	0.0014	3.0872	0.0424	0.2421	0.0028	0.0709	0.0015
HFG-S-16	0.0853	0.0017	2.0093	0.0313	0.1708	0.0020	0.0503	0.0011
HFG-S-17	0.0869	0.0016	2.7988	0.0420	0.2336	0.0026	0.0680	0.0015
HFG-S-18	0.0810	0.0017	2.2069	0.0343	0.1976	0.0022	0.0574	0.0014
HFG-S-19	0.0762	0.0021	1.9939	0.0396	0.1897	0.0021	0.0544	0.0016
HFG-S-20	0.0891	0.0015	2.5110	0.0368	0.2044	0.0023	0.0601	0.0012
HFG-S-24	0.0853	0.0014	2.4996	0.0363	0.2124	0.0025	0.0629	0.0013
HFG-S-27	0.0813	0.0022	2.0642	0.0418	0.1841	0.0021	0.0528	0.0014
HFG-S-28	0.0812	0.0018	2.2283	0.0373	0.1992	0.0023	0.0579	0.0013
HFG-S-3	0.0818	0.0018	2.1921	0.0361	0.1944	0.0022	0.0563	0.0017
HFG-S-6	0.0920	0.0016	3.0655	0.0499	0.2418	0.0028	0.0706	0.0015
HFG-S-8	0.0903	0.0014	3.0360	0.0411	0.2438	0.0025	0.0715	0.0019
HGG-17	0.0727	0.0031	1.3462	0.0491	0.1343	0.0019	0.0397	0.0087
HGG-28	0.0817	0.0014	2.2750	0.0347	0.2021	0.0024	0.0602	0.0021
HGG-7	0.0780	0.0016	2.0987	0.0383	0.1952	0.0021	0.0583	0.0012
HOM-11	0.0904	0.0027	3.1769	0.0816	0.2549	0.0032	0.0714	0.0035
HOM-12	0.0908	0.0020	3.1519	0.0680	0.2518	0.0032	0.0739	0.0021
HOM-13	0.0946	0.0018	3.3077	0.0572	0.2535	0.0031	0.0733	0.0019
HOM-14	0.0953	0.0013	3.5303	0.0460	0.2687	0.0027	0.0782	0.0015
HOM-17	0.0749	0.0030	1.8701	0.0530	0.1811	0.0021	0.0496	0.0023
HOM-18	0.0926	0.0016	3.3075	0.0556	0.2590	0.0031	0.0752	0.0018
HOM-5	0.0863	0.0020	2.7595	0.0522	0.2320	0.0026	0.0670	0.0025
HOM-9	0.0964	0.0015	3.3748	0.0510	0.2540	0.0028	0.0742	0.0017

Table 2 (*continued*)

Analysis	Corrected ratios, $t_2 = 250$ Ma							
	$^{207}Pb/^{206}Pb$ (Ma)	1σ	$^{207}Pb/^{235}U$ (Ma)	1σ	$^{206}Pb/^{238}U$ (Ma)	1σ	$^{208}Pb/^{232}Th$ (Ma)	1σ
JOM-14	0.0818	0.0028	2.3756	0.0660	0.2107	0.0027	0.0597	0.0031
JOM-15	0.0888	0.0025	2.5940	0.0635	0.2120	0.0031	0.0620	0.0028
JOM-3	0.0918	0.0019	3.1965	0.0659	0.2524	0.0035	0.0738	0.0020
JOM-6	0.0915	0.0018	3.1337	0.0564	0.2484	0.0035	0.0721	0.0018
JUS-11	0.0958	0.0019	3.4978	0.0709	0.2647	0.0039	0.0774	0.0025
JUS-2	0.0923	0.0019	3.1052	0.0574	0.2440	0.0029	0.0701	0.0018
JUS-3	0.0922	0.0015	2.8518	0.0427	0.2244	0.0026	0.0658	0.0014
NES-5	0.0904	0.0013	3.1137	0.0399	0.2499	0.0025	0.0732	0.0014
NES-14	0.0949	0.0021	3.3463	0.0682	0.2558	0.0032	0.0743	0.0021
NES-15	0.0972	0.0019	3.5807	0.0617	0.2673	0.0027	0.0761	0.0019
NES-16	0.0959	0.0015	3.5318	0.0520	0.2672	0.0027	0.0776	0.0017
NES-19	0.0954	0.0014	3.4982	0.0509	0.2659	0.0027	0.0775	0.0014
NES-20	0.0945	0.0014	3.3734	0.0486	0.2590	0.0026	0.0758	0.0015
NES-23	0.0971	0.0015	3.6942	0.0549	0.2760	0.0029	0.0804	0.0018
NES-24	0.0965	0.0014	3.5199	0.0518	0.2645	0.0027	0.0772	0.0014
NES-2END	0.0855	0.0018	2.6845	0.0455	0.2276	0.0030	0.0661	0.0017
NES-3	0.0872	0.0018	2.7947	0.0501	0.2325	0.0033	0.0679	0.0021
NES-8	0.0873	0.0018	2.8909	0.0492	0.2401	0.0031	0.0693	0.0020
OE1-1	0.0947	0.0013	3.3543	0.0441	0.2569	0.0027	0.0753	0.0014
OE1-1	0.0947	0.0013	3.3543	0.0440	0.2569	0.0027	0.0753	0.0014
OE1-10	0.0938	0.0014	3.2445	0.0474	0.2508	0.0031	0.0734	0.0016
OE1-10	0.0938	0.0014	3.2441	0.0474	0.2508	0.0031	0.0734	0.0016
OE1-10B	0.0954	0.0014	3.4173	0.0524	0.2597	0.0033	0.0758	0.0018
OE1-10B	0.0956	0.0014	3.4222	0.0519	0.2597	0.0033	0.0758	0.0018
OE1-6	0.0880	0.0015	2.9925	0.0399	0.2468	0.0026	0.0713	0.0017
OE1-8B	0.0951	0.0017	3.0732	0.0487	0.2345	0.0029	0.0680	0.0015
OE1-8B	0.0961	0.0016	3.1043	0.0463	0.2342	0.0029	0.0680	0.0015
OE3-10	0.0879	0.0018	2.3693	0.0397	0.1955	0.0024	0.0571	0.0013
OE3-16	0.0973	0.0014	3.6153	0.0590	0.2695	0.0034	0.0787	0.0018
OE3-19	0.0953	0.0015	3.3638	0.0533	0.2559	0.0033	0.0747	0.0016
OE3-7	0.0950	0.0017	3.2939	0.0571	0.2516	0.0030	0.0735	0.0017
TA116-15	0.0957	0.0019	3.5394	0.0753	0.2682	0.0036	0.0783	0.0018
TA116-19	0.0958	0.0017	3.5380	0.0597	0.2679	0.0032	0.0773	0.0016
TA116-2	0.0985	0.0016	3.5269	0.0594	0.2598	0.0033	0.0754	0.0017
TA116-24	0.0987	0.0014	3.2810	0.0420	0.2411	0.0025	0.0703	0.0012
TA116-9	0.0962	0.0022	3.4225	0.0805	0.2579	0.0036	0.0746	0.0019
TA118-10	0.0927	0.0017	3.2830	0.0575	0.2568	0.0026	0.0747	0.0014
TA118-14	0.0961	0.0018	3.3921	0.0640	0.2559	0.0028	0.0748	0.0014
TA118-15	0.1003	0.0019	3.6965	0.0714	0.2674	0.0033	0.0775	0.0018
TA118-16	0.0966	0.0015	3.4105	0.0545	0.2561	0.0030	0.0748	0.0015
TA118-17	0.0860	0.0022	2.5923	0.0528	0.2186	0.0026	0.0621	0.0017
TA118-19	0.0968	0.0020	3.3964	0.0747	0.2546	0.0031	0.0740	0.0015
TA118-20	0.0970	0.0017	3.3584	0.0560	0.2511	0.0026	0.0730	0.0014
TA118-4	0.0938	0.0018	3.1163	0.0572	0.2410	0.0023	0.0704	0.0013
TA118-8	0.0875	0.0021	2.7883	0.0586	0.2313	0.0028	0.0668	0.0019
TA121-13	0.0877	0.0016	2.8361	0.0456	0.2346	0.0030	0.0683	0.0016
TA121-16	0.0940	0.0014	3.2788	0.0510	0.2530	0.0034	0.0740	0.0016
TA121-4	0.0791	0.0023	1.9533	0.0413	0.1792	0.0023	0.0516	0.0014
TA121-5	0.0860	0.0015	2.2040	0.0319	0.1860	0.0022	0.0548	0.0012
TA121-6	0.0924	0.0012	3.0454	0.0369	0.2391	0.0025	0.0702	0.0012
TRO10-4	0.0957	0.0027	3.2204	0.0854	0.2441	0.0029	0.0712	0.0024

Composition of common lead $^{206}Pb/^{204}Pb = 18.700$ $^{207}Pb/^{204}Pb = 15.628$ $^{208}Pb/^{204}Pb = 38.63$.

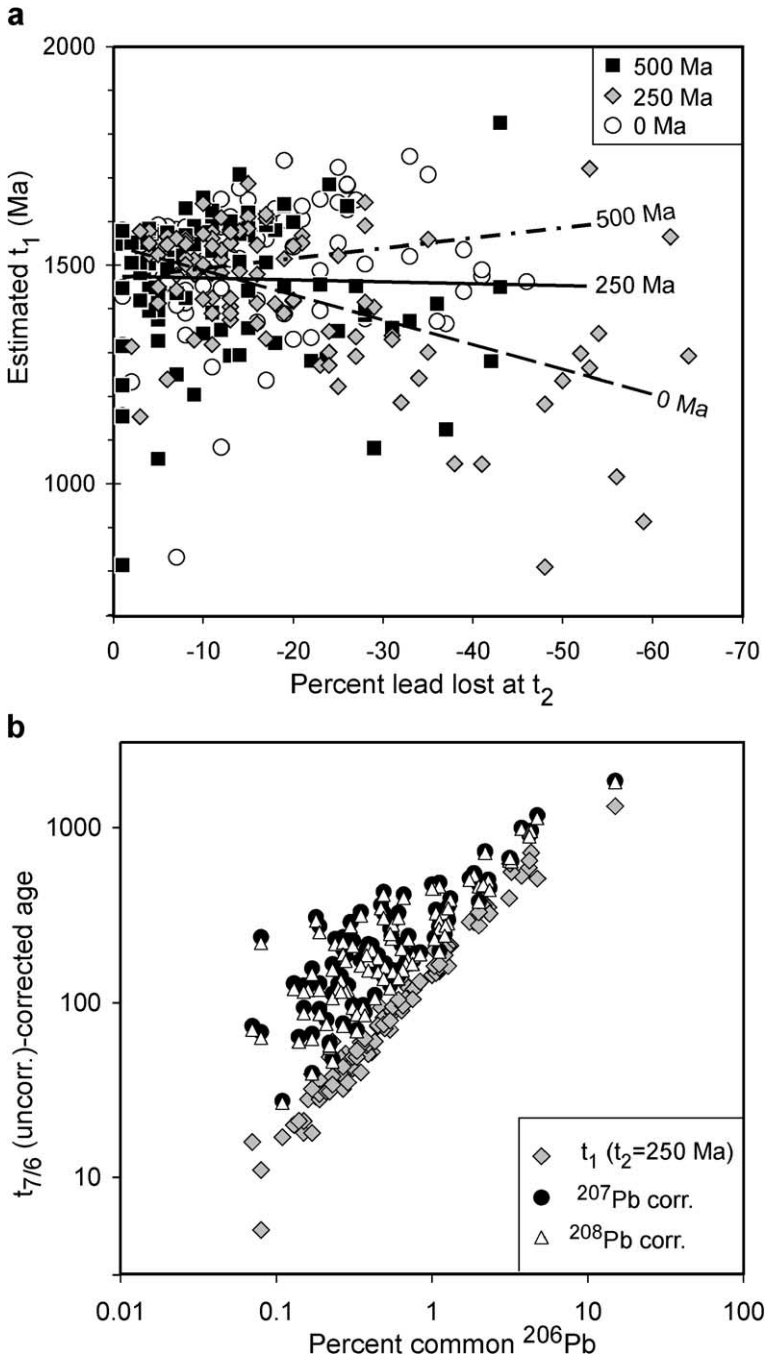

Fig. 5. The effect of common lead correction on analyses of mid-Proterozoic zircons given in Table 2. (a) The effect of correction to lead loss ages (t_2) of 0, 250 and 500 Ma. The straight lines are correlation lines (“trendlines”) calculated for each of the three sets of corrected data. It should be noted that the slope of the line depend on t_2, and that it is close to zero for t_2 = 250 Ma. (b) Correction on the age of zircons as a function of common lead indicated by the present method and by ^{207}Pb and ^{208}Pb corrections.

a systematic *increase* of t_1 with increasing discordance, suggesting that 500 Ma is an overestimate of the age of lead loss. At $t_2 = 250$ Ma, there seems to be little or no systematic shift in t_1 with increasing discordance, indicating that $t_2 = 250$ Ma will induce the least systematic error in t_1. The analyses are therefore recalculated assuming $t_2 = 250$ Ma.

The difference between t_1 and ^{207}Pb and ^{208}Pb corrected ages is shown in Fig. 5b. In general, the present method gives a smaller correction than the ^{207}Pb and ^{208}Pb methods. For this dataset, the latter two methods give nearly indistinguishable results. However, for any range of common lead concentrations from 0.1% to ca. 10%, the ^{207}Pb and ^{208}Pb methods give considerable spread in correction, which is not entirely surprising, as neither of these methods explicitly consider the amount of common lead present in the zircon.

Accumulated probability distribution plots for uncorrected $^{207}Pb/^{206}Pb$ ages, t_1 determined from Eq. (7) and ^{207}Pb and ^{208}Pb corrected ages are shown in Fig. 6. The uncorrected ages give a mid-Proterozoic peak (1.60 Ga), with a small but significant number of points deviating towards higher ages. All correction routines remove the old outliers, and shift the peak of the distribution curve towards lower ages. The present method suggests a peak value at 1.56 Ga, which is compatible with the geological setting of the rocks, and a subsidiary peak of unknown significance at ca. 1400 Ma. Both of these peaks are enhanced when

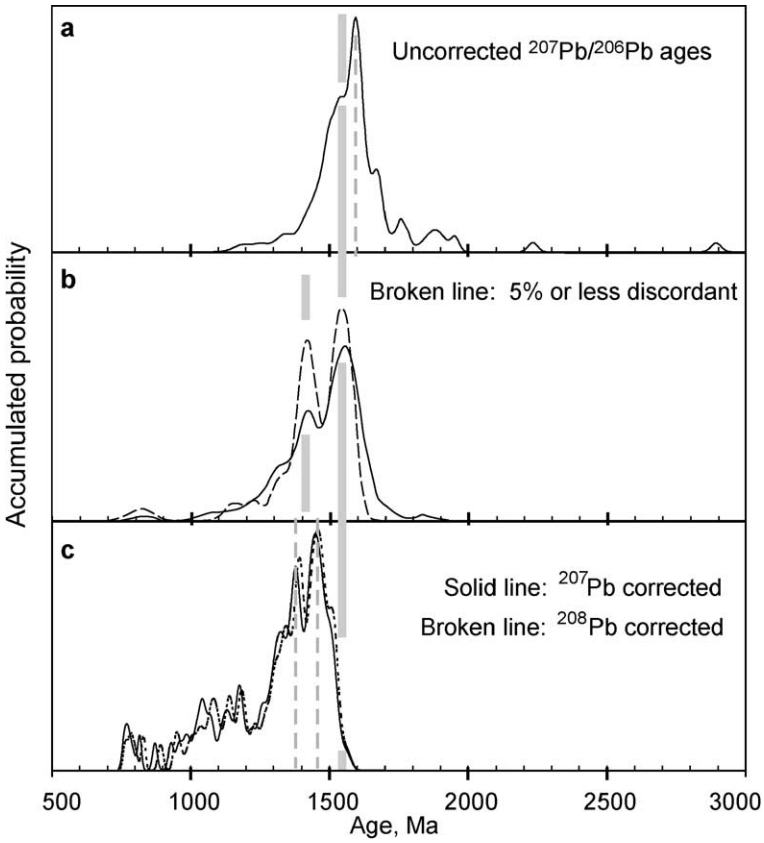

Fig. 6. Accumulated probability curves for mid-Proterozoic zircons, from data in Table 2. (a) Uncorrected data, (b) data corrected by the present method, assuming $t_2 = 250$ Ma and (c) ^{207}Pb and ^{208}Pb corrected data (Isoplot, Ludwig, 2001). The thick, shaded bars represent the most prominent age peaks in the corrected data; the main peak at 1560 Ma corresponds to the preferred initial crystallization age of the zircons. The thinner, broken, vertical lines represent the respective frequency peaks in uncorrected data (a) and ^{207}Pb and ^{208}Pb corrected data (c).

only grains 5% or less discordant are considered, but their positions are not affected. The ^{207}Pb and ^{208}Pb corrections shift the position of the main peak to 1.46 Ga, which is well after the end of active subduction in the region, and therefore incompatible with regional geology.

The ^{207}Pb and ^{208}Pb corrections also yield a number of subsidiary peaks at $t<1200$ Ma, which reflect strongly discordant grains which are significantly overcorrected. The t_1 curves have much less pronounced low-age tails, suggesting that meaningful, corrected ages can be extracted even from grains which are quite strongly discordant.

4.4. Recommendations

If data on ^{204}Pb are unavailable, the method outlined in this paper can provide realistic corrections for common lead. However, the method should not be used uncritically. Points to keep in mind are the composition of the common lead and the timing of the lead-loss event. If the composition of the common lead is known, for example, by analysis of galena or potassium feldspar coexisting with the zircon, this composition would normally be representative of the common lead composition at the time of crystallization. However, in LAM-ICPMS analysis, there is a danger that lead contained in the mounting medium may contribute to the analysis, especially for small grains and towards the end of a time-resolved run. If the lead isotopic composition of the epoxy is known from analysis, its composition may be used. If no data on the composition of the actual common lead present are available, a model composition representing average crustal lead could be substituted. The global second-stage reservoir of Stacey and Kramers (1975), characterized by present-day $^{206}Pb/^{204}Pb=18.700$, $^{207}Pb/^{204}Pb=15.628$, $^{208}Pb/^{204}Pb=38.63$, $^{238}U/^{204}Pb=9.74$, $^{232}Th/^{204}Pb=36.84$ and $^{232}Th/^{238}U=3.78$ provides frequently used reference values for common lead, which may be used equally well in the present method. At least for post-Archaean systems, choice of an inappropriate age on this curve (e.g. the present-day composition instead of the composition at the time of crystallization) would cause a systematic, but in most cases insignificant, bias in the result.

The need to know the age of lead loss (t_2) is a limiting factor for the use of the method. If t_2 can be constrained from independent data, this age should be used. Otherwise, t_2 should be selected so that the resulting bias in t_1 is as small as possible, preferably within the error caused by the $\pm 2\sigma$ error on the corrected isotopic ratios. In most cases, assuming a t_2 older than its real age has more damaging effects than an underestimate of t_2. Some constraints on t_2 can be obtained by considering the relationship between the discordance of the corrected lead isotope compositions and the corrected ages for a population of approximately coeval zircons. Estimates of t_1 can easily be made at different choices for t_2, and the t_2 value which induces little or no change in t_1 with increasing discordance is likely to cause least systematic error in t_1, and should be preferred for the population as a whole.

Zircons which have not lost lead will yield corrections equivalent to those made by the ^{207}Pb method. The advantage of the present method is that it actually demonstrates rather than assumes such concordance.

Grains which appear to have suffered U/Th differentiation at a late stage in their history should be treated with extreme care; such zircons can in principle only be corrected by the ^{207}Pb method, which is likely to give an underestimate of the real age.

In any case, it is important to remember that the fight against common lead starts in the laboratory, and that efforts must be made to remove common lead from grain surfaces and fractures, and to use mounting and polishing media with minimal Pb content. Furthermore, if LAM-ICPMS data are processed in time-resolved mode, care should be taken to avoid any part of a signal that shows irregular fluctuations in any of the lead isotope signals, and, in particular, those which show anomalous increases in ^{208}Pb.

5. Conclusions

LAM-ICPMS U–Pb analyses of zircons and other U-enriched minerals which do not include data on ^{204}Pb can be corrected for common lead. The method developed in this paper assumes that the discordance of Pb/U and Pb/Th isotopic ratios observed in a zircon is a sum of the effects of common lead contamination and lead loss. The radiogenic lead component in the zircon

and its initial age can be determined by the simultaneous solution of six equations in the six variables describing the mass balance of a discordant zircon which contains common lead and which has suffered partial lead loss in an event after initial crystallization (initial age (t_1), $^{206}Pb_r/^{238}U$, $^{207}Pb_r/^{235}U$, $^{208}Pb_r/^{232}Th$, fraction of common ^{206}Pb and fraction of lead lost). The time of the lead loss event (t_2) must be assumed or constrained by additional data. The bias in t_1 introduced by an erroneous choice of t_2 will exceed the 2σ error interval of t_1 caused by analytical error only when the assumed t_2 differs from the correct value by several hundred million years.

The strength of this method is that it does not rely on data for a minor isotope, which cannot be measured in some instrumental methods. The main weakness is that the age of lead loss must be constrained by external data, but for most common lead-bearing zircons for which ^{204}Pb is not reported, the correction method suggested here is likely to give a less biased age than the alternative methods available.

Acknowledgements

Thanks are due to S.Y. O'Reilly and W.L. Griffin for invitations to two extended visits to GEMOC, Maquarie University, in 2000 and 2001, during which this work was done. Travel costs were covered by grants from the Faculty of Mathematics and Natural Sciences, University of Oslo, and from the Norwegian Research Council. The study has benefited greatly from discussions with Bill Griffin, Simon Jackson, Norman Pearson, Elena Belousova and Chris Ryan, and from reviews by Kenneth R. Ludwig and anonymous referee. **[RR]**

References

Andersen, T., Griffin, W.L., Jackson, S.E., Knudsen, T.-L., 2001. Timing of mid-Proterozoic calcalkaline magmatism across the Oslo Rift: implications for the evolution of the southwestern margin of the Baltic Shield. Geonytt 1, 25–26.

Andersen, T., Griffin, W.L., Pearson, N.J., 2002. Crustal evolution in the SW part of the Baltic Shield: the Hf isotope evidence. Journal of Petrology 43, No. 9 (September).

Bingen, B., van Breemen, O., 1998. Tectonic regimes and terrane boundaries in the high-grade Sveconorwegian belt of SW Norway inferred from U–Pb zircon geochronology and geochemical signature of augen gneiss suites. Journal of the Geological Society, London 155, 143–154.

Connelly, J.N., Åhäll, K.I., 1996. The Mesoproterozoic cratonization of Baltica; new age constraints from SW Sweden. In: Brewer, T.S. (Ed.), Precambrian Crustal Evolution in the North Atlantic Region. Geological Society Special Publications, London, pp. 261–273.

Dickin, A.P., 1995. Radiogenic Isotope Geology Cambridge Univ. Press, Cambridge. 490 pp.

Faure, G., 1986. Principles of Isotope Geology, 2nd ed. Wiley, New York. 555 pp.

Lee, J.K.W., Williams, I.S., Ellis, D.J., 1997. Pb, U and Th diffusion in natural zircon. Nature 390, 159–162.

Ludwig, K., 1980. Calculation of uncertainties of U–Pb isotope data. Earth and Planetary Science Letters 46, 212–220.

Ludwig, K., 2001. Isoplot/Ex, rev. 2.49. A Geochronological Toolkit for Microsoft Excel. Berkeley Geochronology Center, Berkeley, CA, USA, Special Publication No. 1a.

Nordgulen, Ø., Tucker, R.D., Sundvoll, B., Solli, A., Nissen, A.L., Zwaan, K.B., Birkeland, A., Sigmond, E.M.O., 1997. Paleo- to Mesoproterozoic intrusive rocks in the area between Numedal and Mjøsa, SE Norway. In: Nordgulen, Ø., Padget, P., Robinson, P., McEnroe, S. (Eds.), COPENA Conference at NGU, August 18–22, 1997: Abstracts and Proceedings. Norges geologisk Undersøkelse Report.

Sigmond, E.M.O., 1998. Geologisk kart over Norge, Berggrunnskart ODDA, M 1:250 000. Norges geologisk undersøkelse, Trondheim.

Stacey, J.S., Kramers, J.D., 1975. Approximation of terrestrial lead isotope evolution by a two-stage model. Earth and Planetary Science Letters 26, 207–221.